Arabian Journal of Chemistry (2022) **15**, 103941

King Saud University

Arabian Journal of Chemistry

www.ksu.edu.sa
www.sciencedirect.com

ORIGINAL ARTICLE

Exploring the interaction of sesamol as an antilung cancer compound with albumin through spectroscopic and bioinformatic analyses and the mechanism of anticancer effect

Liya Hu [a,1], Hong Cao [a,1], Bangshun He [b,1], Lijun Zheng [a], Ruichao Li [a,*]

[a] *Geriatric Department of Tongji Hospital, Tongji Medical College, Huazhong University of Science and Technology, Wuhan 430030, China*
[b] *Oncology Department of Tongji Hospital, Tongji Medical College, Huazhong University of Science and Technology, Wuhan 430030, China*

Received 24 February 2022; accepted 21 April 2022
Available online 4 May 2022

KEYWORDS

Sesamol;
Human serum albumin;
Interaction;
Lung cancer cells

Abstract Sesamol has moved into biomedical research in recent years. However, its interactions with blood proteins and cancer cells have not been fully explored. Therefore, we aimed to investigate the interaction of sesamol with human serum albumin (HSA), A549 human nonsmall cell lung cancer (NSCLC) cell line, and Raw 264.7 macrophage. The interaction of HSA with sesamol was explored via application of fluorescence and circular dichroism (CD) spectroscopy studies as well as molecular docking analysis. Then, the cytotoxic effects of sesamol on A549 lung cancer cells and Raw 264.7 macrophages were evaluated by qPCR analysis. It was found that sesamol spontaneously (ΔG°=-45.89 kJ/mol) binds with HSA having a high affinity (log K_b = *8.05*, n = *1.70*, T = *298 K*) and form a static complex trough contribution of hydrogen bonds and van der Waals interactions (ΔH°=-409.43 kJ/mol, $T\Delta S^{\circ}$=-363.54 kJ/mol) which was supported by molecular docking study. Furthermore, by using CD and synchronous fluorescence spectroscopy analyses it was found that sesamol induced some minor secondary and tertiary structural changes, respectively in HSA structure. Cellular assays displayed that sesamol triggered selective cytotoxicity against A549 lung cancer cells through regulation of intrinsic apoptosis pathway mediated by mitigation of mitochondrial membrane potential, elevation of ROS generation, downregulation of Bax, and

* Corresponding author at: Department of General Medicine, Tongji Hospital, Tongji Medical College, Huazhong University of Science and Technology, NO.1095, Jiefang Avenue, Wuhan 430030, China.
E-mail address: r461791@yahoo.com (R. Li).
[1] Contributed equally to this study.

Peer review under responsibility of King Saud University.

Production and hosting by Elsevier

https://doi.org/10.1016/j.arabjc.2022.103941

up regulation of caspase-9, −3. In conclusion, it was found that sesamol could show high affinity with HSA and mediate intrinsic apoptosis pathway through ROS generation in the A549 lung cancer cell lines. These data indicate that the biochemical and anticancer mechanisms of sesamol can be further investigated in future studies to integrate it in the biomedical platforms.

1. Introduction

Sesamol ($C_7H_6O_3$) as a natural organic molecule is widely found in sesame seeds and oil (Bosebabu et al. 2020). It is one of the most widely studied small molecules for biomedical applications in vitro and *in vivo* (Bosebabu et al. 2020). For example, it has been shown that sesamol can show antioxidant (Zhou et al., 2021), neuroprotective (Abou-Zeid et al. 2021), and anticancer activities (Majdalawieh and Mansour, 2019; Abd Elrazik et al. 2021).

It has been revealed that the pharmacodynamic and the metabolism of different small molecules may be heavily influenced by ligand-receptor interactions (Mealey and Karriker, 2019). This kind of interaction can also affect the small molecule stability and free concentration in the tissues. Human serum albumin (HSA) with dominant α-helix structure is one of the most abundant proteins in blood, which show several physiological actions including the regulation of blood pressure and pH, drug interactions, and drug carriers (Carter et al., 1989). Indeed, several small molecules can bind reversibly with HSA as a carrier which result in the apparent solubility of drugs in plasma (Beigoli et al. 2019; Sułkowska, 2002). Therefore, it is vital to explore the bioaffinity of a small molecule with HSA, even if it is not the only approach to examine serum concentrations of the free small molecules.

On the other hand, it has been shown that sesamol has anticancer effects against multiple types of cancers in vitro (Majdalawieh et al. 2019 Abdelhamid et al. 2019). For example, it has been shown that sesamol has the ability to induce apoptosis in hepatic cell line (Liu et al., 2013), block cyclooxygenase-2 transcriptional activity (Shimizu et al., 2014) and regulate mitochondrial apoptosis pathway in colon cancer cells (Khamphio et al., 2016), and upregulate miR-370-3p in breast cancer cells (Ma et al., 2021).

In the following decades, nonsmall cell lung cancer (NSCLC) increased dramatically due to air pollution and lifestyle (Hackshaw et al., 1997). Lung cancer is the leading cause of cancer death in men and women worldwide (McIntyre and Ganti, 2017). It has been reported that lung cancer spreads or metastasizes rapidly after formation and is one of the most incurable cancers. The adrenal glands, liver, brain and bones are the most common sites for lung cancer metastasis (Shroff et al., 2018).

Although, it has been shown that sesamol can induce apoptotic effect in lung cancer cells through different pathways (Siriwarin and Weerapreeyakul, 2016), the possible mechanism of anticancer effect of sesamol against A549 human nonsmall cell lung cancer (NSCLC) has not been fully explored in detail.

The internal pathway of apoptosis is activated by a wide range of factors such as hypoxia, DNA damage, and reactive oxygen species (ROS) mediated by Bcl-2 and caspase family proteins (Jendrossek, 2012).

Hence in this study we aimed to first determine the affinity of HSA with sesamol through different spectroscopic and in silico studies. Afterwards the anticancer mechanism of sesamol against A549 human nonsmall cell lung cancer cells was explored by different cellular and molecular assays to investigate the possible apoptosis mediated by intrinsic apoptosis pathway.

2. Materials and methods

2.1. Materials

Sesamol and human serum albumin (HSA) were obtained from Sigma (Shanghai, China). The materials were dissolved in Tris–HCl buffer solution (50 mM Tris–Base, 100 mM NaCl, pH 7.4). The sample solutions were only prepared just before assay. All solutions were prepared with double distilled water.

2.2. Fluorescence experiment

All fluorescence spectra were read using a F-2500 spectrofluorimeter, where the circulating bath (Hitachi, Japan) was employed to control the temperature of the system. Fluorescence assays were done at three different temperatures (298, 310, and 315 K), where the protein concentration was fixed at 2 μM and the sesamol concentrations were used in the range of 5 μM to 40 μM. The excitation wavelength was set at 295 nm and the excitation and emission slit widths were fixed at 5 nm. For synchronous fluorescence spectroscopy, the $\Delta\lambda = 60$ nm and $\Delta\lambda = 15$ nm were used to explore the microenvironmental changes around tryptophan (Trp) and tyrosine (Tyr) residues, respectively. The samples were corrected against control, sesamol, and inner filter effect (Abdollahpour et al. 2016).

2.3. Circular dichroism (CD) study

CD spectra were read using a Jasco J-810 spectropolarimeter with a 1 mm cell at ambient temperature. Scans were made from 190 to 260 nm, with a scan rate of speed of 200 nm/min. The protein concentration was 10 μM and the sesamol concentrations were used in the range of 5 μM to 40 μM. The data were reported as Mean Residue Ellipticity (MRE) in deg. cm^2 $dmol^{-1}$.

2.4. Molecular docking analysis

The structure of HSA was downloaded from the PDB (PDB ID: 6HSC) with a resolution: 1.9 Å and water molecules were replaced with hydrogens along with the Kollman charges by using MGL software (Jacob et al., 2012; Abd-Algaleel et al. 2021). To parameterize the sesamol ligand, the Antechamber software along with Polak–Ribiere conjugate gradient algorithm were used. Grid box with a space of 1 Å was designed and the box was created with dimensions of 76* 46 * 76 Å. The interaction of HSA with sesamol was explored while using VMD visualizer.

2.5. Cell culture

A549 human nonsmall cell lung cancer (NSCLC) cell line and Raw 264.7 macrophage cells obtained from ATCC (Shanghai, China) were cultured in RPMI-1640 culture medium Gibco, Shanghai, china) supplemented with 10% fetal bovine serum (FBS) Gibco, Shanghai, China), 2 mM L-glutamine (Hi Media, Mumbai, India), and 1x penicillin (Hi Media, Mumbai, India), streptomycin, and neomycin (Hi Media, Mumbai, India).

2.6. MTT assay

Cell lines (1×10^5 cells per well) were seeded (96-well plate), incubated for 24 h, and exposed to different concentrations of sesamol (1–1000 μM) for 24, where the cells without sesamol were considered as control. Then, the cells were added by 20 μl of MTT solution (5 mg/ml) and incubated for 4 h. The culture medium was then gently removed and replaced with 100 μl of DMSO for 5 min. Absorbance was finally read at 570 nm using an ELISA plate reader.

2.7. Analysis of mitochondrial membrane potential (MMP)

MMP was quantified using the JC-1 probe (Beyotime, China). Cells incubated with a fixed (IC_{50}) concentration of sesamol for 24 h and were then added by 5 μg/mL JC-1 for 30 min at 37 °C, followed by washing with PBS. Afterwards, fluorescence intensity was read on a multimode microplate reader (Bio-Rad). The samples were excited at 485 nm, and the emission was read at 585 and 538 nm. The data was expressed as the OD585/OD538 ratio.

2.8. Analysis of reactive oxygen species (ROS)

ROS production in the cells was determined using the 2′,7′–dichlorofluorescin diacetate (DCFDA) ROS assay kit (ab113851) based on the manufacturer's protocols. Cells incubated with a fixed (IC_{50}) concentration of sesamol for 24 h and then added by 10 μg/mL DCFDA for 30 min at 37 °C, followed by washing with PBS. Fluorescence intensity was then read on a microplate reader (Bio-Rad) at excitation / emission of 485 nm / 535 nm.

2.9. Gene expression assay

Expression of apoptosis related genes, Bcl-2, Bax, caspase-9, and caspase-3 was analyzed using quantitative real time-PCR (qPCR). The housekeeping gene GAPDH was used as control. Total RNA was extracted with a trizol reagent (Invitrogen, China). cDNA was then produced by reverse transcription of denatured RNA (3 μg) at 37 °C for 1 h using Reverse Transcriptase kit (Invitrogen, China). The PCR reaction was done based on the previous study (https://www.sciencedirect.com/science/article/pii/S0304383504000539).

The primers used for this study were summarized in Table 1.

Primer	Forward	Reverse
GAPDH	5′- CGACCACTTTG TCAAGCTCA-3′	5′- CCCCTCTTCAAGGG GTCTAC-3′
Bcl-2	5′- GATTGTGGCCT TCTTTGAG-3′	5′- CAAACTGAGCA GAGTCTTC-3′
Bax	5′- GCCCTTTTGCT TCAGGGTTT-3′	5′- TCCAATGTCCA GCCCATGAT-3′
Caspase-9	5′-CTGTCTACG GCACAGATGGAT-3′	5′-GGGACTCGTCT TCAGGGGAA-3′
Caspase-3	5′-AGAACTGGACT GTGGCATTGAG-3′	5′- GCTTGTCGGCA TACTGTTTCAG-3′

2.10. Caspase activity assay

Caspase-9 and −3 activities were assessed in A549 cells after exposure to sesamol (IC_{50} concentration) for 24 h using caspase-9 assay kit (E-CK-A313, Elabscience) and caspase-3 assay kit (E-CK-A311, Elabscience) based on the manufacturer's protocols. Briefly, after cell lysis and centrifugation for 1 min at 10,000 × g at 4 ℃, 100 μl of cell lysate was added by equal volumes of reaction buffer. Thereafter, 4 mM substrates were added and incubated for 10 min. Finally, the absorbance of the samples was read at 405 nm using a microplate reader.

2.11. Statistical analysis

All data were reported as mean ± SD and statistical analyses were done using ANOVA and student's 't' test. Blank samples corresponding to the sesamol and buffer were subtracted to correct background spectra and cytotoxicity. $P < 0.05$ were considered statistically significant.

3. Results and discussions

3.1. Fluorescence spectra and quenching mechanism

Fig. 1a displays the emission spectra of HSA with various concentrations of sesamol. It was found the fluorescence intensity of HSA reduced regularly with the increasing of sesamol concentration. Indeed, fluorescence quenching method is a widely used approach to explore the binding affinity of small molecules with proteins (Wang et al. 2006; Ziaunys et al. 2019).

We performed the study within the linear part of Stern–Volmer (SV) plot:

$$F_0/F = K_{SV}[Q] + 1 = kq\tau o[Q] + 1 \quad (1)$$

Where F_0, F, K_{SV}, Q, kq, and τo are the fluorescence intensity without quencher, fluorescence intensity with quencher, SV coefficient, concentration of quencher, bimolecular quenching constant, and fluorescence emission time, respectively (Mahmoudpour et al., 2020).

Table 1 Quenching, binding and relative thermodynamic parameters upon interaction of HSA with sesamol.

T (K)	K_{sv} (10^5, M^{-1})	k_q (10^{14}, M^{-1} s^{-1})	R^2	log K_b (M^{-1})	n	R^2	ΔH (kJ/mol)	TΔS (kJ/mol)	ΔG (kJ/mol)
298	1.24	1.24	0.98	8.05	1.70	0.94	−409.43	−363.54	−45.89
310	0.79	0.79	0.96	5.34	1.14	0.96	−409.43	−378.18	−31.25
315	0.33	0.33	0.97	4.14	0.99	0.94	−409.43	−384.27	−25.15

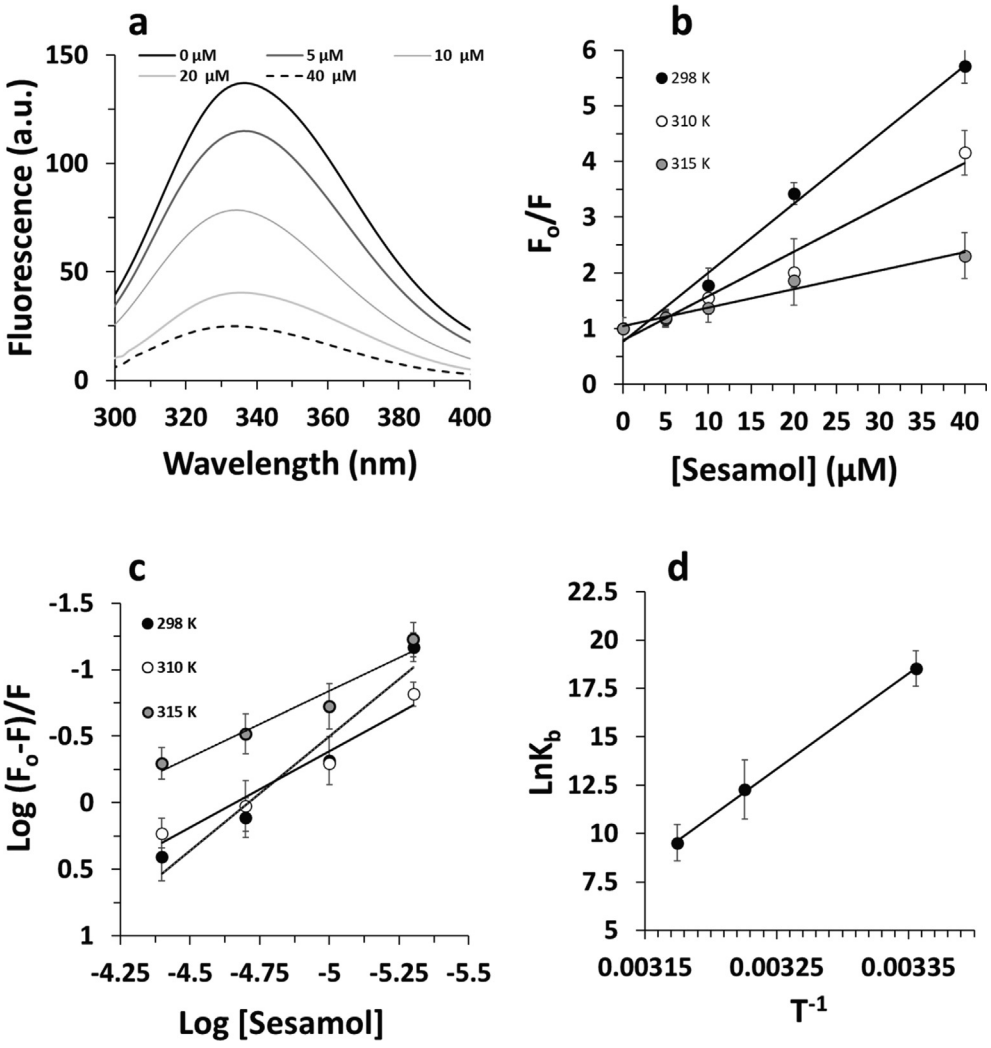

Fig. 1 (a) Emission spectra of HSA with different concentrations of sesamol (T = 298 K). [HSA] = 2 μM; [Sesamol] (5–40 μM), (b) Stern-Volmer (SV) plot for the interaction of HSA with sesamol, (c) modified SV plot for determining the binding parameters, (d) van't Hoff plot for determining the thermodynamic parameters.

For this assay the concentration of HSA was fixed at 2 μM and the concentrations of sesamol were in the range of 5 to 40 μM.

It has been reported that quenching can happen by two main mechanisms, which normally categorized as dynamic and static quenching classified by their dependence on temperature. Higher temperatures lead to induction of a faster diffusion and the dissociation of weekly formed ligand-receptor complexes, resulting in a smaller amount of static quenching (Abdelaziz et al., 2021).

Fig. 1b displays the SV plots of the quenching of HSA fluorescence by sesamol at different temperatures (298, 310, 315 K). The corresponding K_{SV} at different temperatures are summarized in Table 1.

These data indicated that the possible quenching mechanism of HSA fluorescence by sesamol is a static quenching process, because the K_{SV} values decreased with the temperature of the system rising. Also, it was shown that the amount of kq was about 1.24×10^{14}, which was much higher than that of the dynamic complex formation (10^{10}) (Nakhjiri et al., 2020).

3.2. Analysis of binding equilibria

When a small molecule interacts independently with a biomacromolecule, the equilibrium between free and bound small molecule is depicted by the following modified SV equation (Macii et al. 2021):

$$logF_0 - F/F = logKb + nlog[Q] \quad (2)$$

where, K_b is the binding constant and n is the number of binding sites per receptor.

Fig. 1c and Table 1 display the outcomes at three different temperatures assessed in this way for interaction of HSA with sesamol. The R^2 values were > 0.93, revealing that the expectations underlying the derivation of the modified SV equation are satisfactory. Table 1 displays the data of K_b and n values which reduced apparently with the temperatures rising, indicating the significant decomposition of sesamol-HSA complex at higher temperatures, hence, K_b values reduced markedly with the increase of temperatures. Furthermore, it should be noted the high value of K_b indicates that a possible interaction between sesamol and HSA can occur *in vivo* (Baghaee et al. 2019).

Also, it was deduced that there is sesamol molecular binding with HSA according to approximately 2:1 (sesamol: HSA).

In general, K_{SV} and K_b are indicative of the aromatic residue accessibility and binding affinity upon interaction of small molecules and proteins.

3.3. Binding forces

The type of interaction of a small molecule and protein can be influenced by several parameters including stereoeffect, hydrophobicity, polarity, and etc. (Afkham et al., 2022). Through a thermodynamic system the main interaction force between a ligand and a receptor can be determined. That is why, the temperature-dependence of the K_b was investigated. Indeed, free HSA does not display any structural changes at the three chosen temperatures 298, 310 and 315 K.

A plot of $\ln K_b$ versus $1/T$ yields a straight line based on the van't Hoff equation (Afkham et al. 2022):

$$lnK_b = -\Delta H^\circ/RT + \Delta S^\circ/R \quad (3)$$

Then, values of enthalpy charges (ΔH) and entropy changes (ΔS) can be calculated from the slop end Y-interpret of van't Hoff plot, respectively (Fig. 1d). Afterward, free energy change (ΔG) can be calculated based on the following relationship:

$$\Delta G^\circ = \Delta H^\circ - T\Delta S^\circ \quad (4)$$

Table 1 also summarizes the values of ΔH and $T\Delta S$ and ΔG determined based on the Fig. 1d.

From Table 1, it can be deduced that the negative sign for ΔG indicates that the interaction between sesamol and HSA is spontaneous (Zeinabad et al. 2016). The negative ΔH and ΔS values reveal that the interaction is mostly enthalpy-driven and the entropy is unfavorable for this interaction, thus the hydrogen bonds or van der Waals forces play a key role in the interaction (Zeinabad et al. 2016).

It has been found that binding affinity and kind of interactions for some known anticancer small molecules like curcumin (n = 1, K_b = 5.46 × 10^4, hydrophobic interactions) (Ge et al., 2014), safranal (n = 1.28, K_b: 1.23 × 10^4, hydrophobic and hydrogen bonding interactions) (Salem et al., 2019), crocin (n = 1.4, K_b = 3.25 × 10^3, hydrophobic and hydrogen bonding interactions) (Salem et al. 2019), enasidenib (n = 1.04, K_b = 9.76 × 10^4, electrostatic interactions) (Abdelhameed et al. 2022) are different from those of sesamol. Indeed, it should be noted the presence of phenol and methylenedioxy in sesamol structure can result in the higher affinity and potential interaction of HSA with sesamol.

3.4. Exploring the microenvironmental changes around aromatic residues

Synchronous fluorescence spectroscopy (SFS) a sensitive technique for the analysis of microenvironmental changes around Trp and Tyr residues was used to assesses the probable changes around this residue (Abdolmajid et al., 2019; Arsalan et al. 2020). Therefore, in this assay, we tried to analyze the interaction between sesamol and HSA by SFS. For SFS analysis, $\Delta\lambda$ = 60 nm and $\Delta\lambda$ = 15 nm can be used to determine the microenvironmental changes around Trp and Tyr residues, respectively. As it was shown in Fig. 2, as the concentration of sesamol increased, a reduction in the intensity of both Trp (Fig. 2a) and Try (Fig. 2b) residues were observed. However, there was a red-shift in the maximum wavelength of Trp residue (Fig. 2a), indicating the probable microenvironmental changes around this residue and displacement toward a more hydrophilic environment (Li et al., 2022).

3.5. Investigation of the secondary structure of HSA upon interaction with sesamol

CD spectroscopy is known as a sensitive tool to analyze structural changes taking place in a biomolecule after interaction with a ligand. The interaction of small molecules to proteins influences the intermolecular forces mediating the stability of the protein structures, which if changed lead to conformational alteration of the proteins. When a small molecule binds with the protein, it leads to structural changes in protein reflected by CD spectra. Fig. 2c depicts the far UV CD signals of HSA with and without different concentrations of sesamol. It is evident from the Fig. 2c that slight alterations occur in CD spectra of HSA. Native HSA with 2 minima at 208 nm and 222 nm, the characteristics of α-helix structure, does not experience a substantial structural change upon addition of varying concentrations of sesamol evident from the minimum changes in two minima at 208 and 222 nm. For the free HSA, the %α-helix as determined by the CD software was found to be 53.97% while after the addition of the highest concentration of sesamol (40 μM), there was a slight reduction in %α-helix and it was determined to be 48.01%, revealing that protein has functionally a-helix even after interaction with sesamol. In general, small molecule-protein interaction probably alters the intermolecular forces responsible for stabilization of the secondary structures causing conformational changes in protein.

It has been found that some other small anticancer molecules including (−)-epigallocatechin-3-gallate (Maiti et al., 2006), tea polyphenols (Bose et al. 2016), and embelin (Yeggoni et al., 2016).

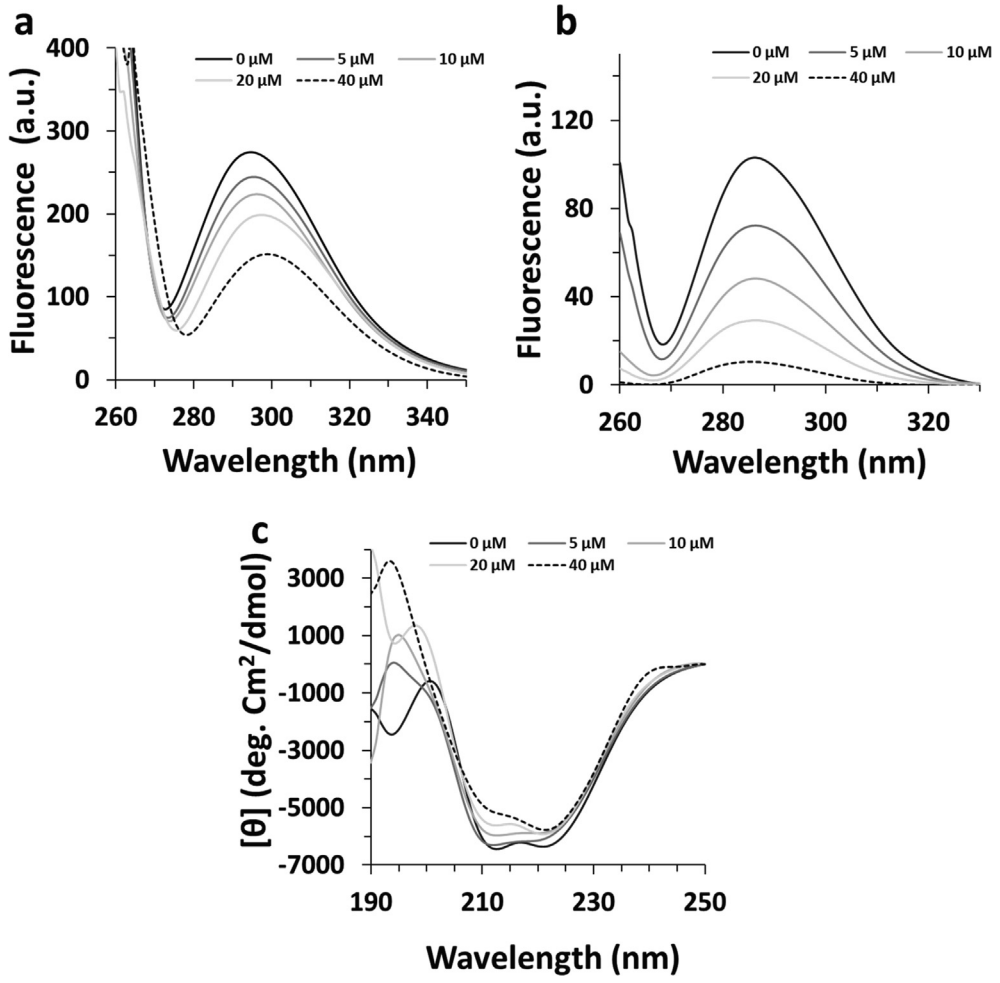

Fig. 2 Synchronous fluorescence spectroscopy for determination of microenvironmental changes around (a) Trp residue at $\Delta\lambda = 60$ nm and (b) Tyr residues at $\Delta\lambda = 15$ nm. Emission spectra of HSA were read with different concentrations of sesamol ($T = 298$ K). [HSA] = 2 μM; [Sesamol] (5–40 μM). (c) CD spectra of HSA with and without different concentrations of sesamol for determining the secondary structural changes. Ellipticity spectra of HSA were read with different concentrations of sesamol ($T = 298$ K), [HSA] = 10 μM; [Sesamol] (5–40 μM).

3.6. Molecular docking study

Molecular docking analysis was done by 3 clusters of sesamol and it was found that they can bind with HSA with notable binding affinities of −6, −5.44, −5.43 kcal mol^{-1} for cluster 1, 2, 3, respectively (Fig. 3a). As cluster 1 showed the most binding energy, the further in silico studies were done on this cluster. Interaction analysis indicated that sesamol is binding into the functionally active residues. The chemical structure of sesamol and its binding ability with HSA is displayed in Fig. 3a and the involved residues in the binding pocket are shown in Fig. 3b. Some active residues of HSA including Leu213, Trp214, Leu481, Phe206, Ala210, Gly207, Ser202, and Phe211 in subdomain IIA are involved in main interactions with sesamol, where Ser202 shares hydrogen bond (green dashed line) and the other amino acid residues share van der Waals interactions (red semicircle line) (Fig. 3b) which is in good agreement with fluorescence quenching study. Indeed, sesamol ligand is able to bind at the comparable site where some other small molecule including prometryn (Wang et al., 2014), cefodizime (Hu and Liu, 2015), trelagliptin (Gan et al., 2018), dolutegravir intermediate (Behera et al. 2021), and esculin (Qureshi et al., 2022) bind with HSA. Indeed, sesamol mimics the similar pose of above-structures and binds in the comparable site indicating the importance of this interaction.

3.7. Sesamol mitigated cell viability

Previous studies revealed that sesamol mitigated cell viability and triggered apoptosis in cancer cells (Liu et al., 2017). Here, we also assessed the anticancer effect of sesamol against A549 cells. It was found that sesamol notably reduced A549 cells viability in a dose-dependent fashion with much lower toxicity on normal Raw 264.7 macrophage cells (Fig. 4a). Also, it was shown that the IC_{50} concentration of sesamol against A549 and Raw 264.7 cells were 501 ± 33.83 μM and > 1000 μM, respectively. In a previous report it has been shown that IC_{50} concentration of sesamol against human hepatoma cells

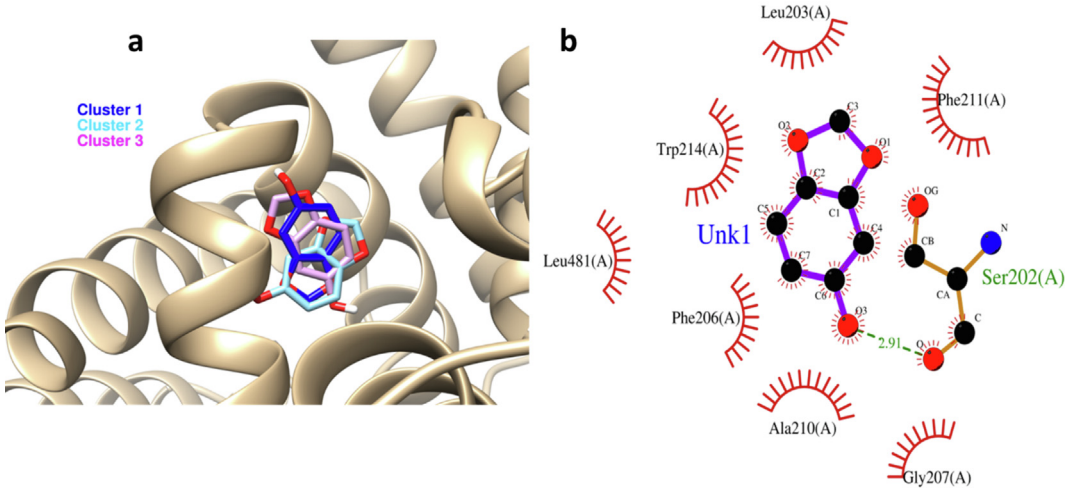

Fig. 3 (a) exploring the interaction of 3 designed clusters of sesamol by molecular docking study. (b) Visualization of docking site by VMD graphical software. Green line: hydrogen bonds, red semicircle: van der Waals forces.

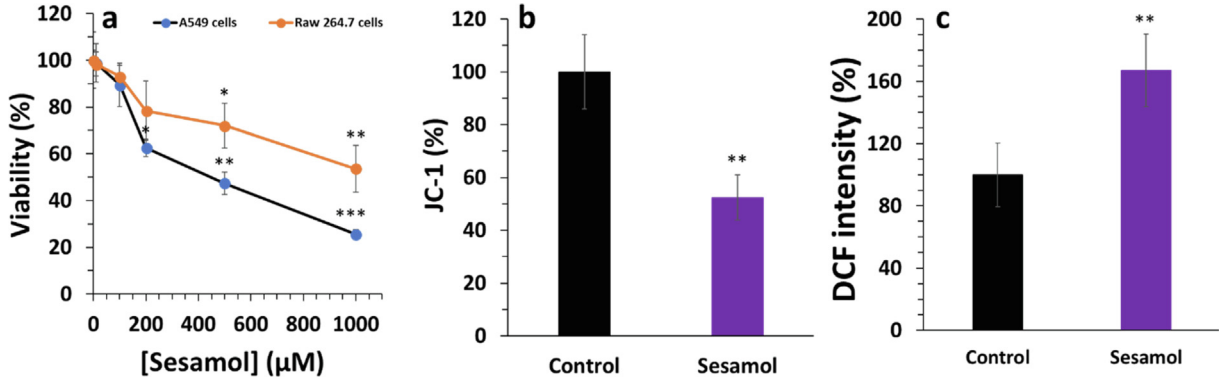

Fig. 4 (a) MTT assay of cells treated with different concentrations of sesamol for 24 h, (b) Sesamol (IC_{50} concentration) mitigated the mitochondrial membrane potential in A549 ling cancer cells after 24 h evidenced by JC-1 fluorescence assessed by a fluorometer, (c) Sesamol (IC_{50} concentration) increased the ROS level after in A549 lung cancer cells after 24 h evidenced by dichlorofluorescein (DCF) fluorescence intensity assessed by a fluorometer. Data presented as mean ± SD, n ≥ 3, *P < 0.05, **P < 0.01, ***P < 0.001 versus blank treatment group.

(HepG2) and normal hepatocytes BRL-3A were 480 μM and > 1000 μM, respectively (Liu et al. 2017). In another study, it was revealed that the determined IC_{50} was 885 μM ± 15.21 for the sesamol aqueous solution against MCF-7 breast cancer cells (ElMasry et al., 2018). In another study, different sesamol derivatives were synthesized and their anticancer effects against A549, MCF-7, and HeLa cells were investigated. It was seen that the IC_{50} concentrations can be varied in the range of 42 μg/ml to > 1000 μg/ml based on the type of the cells and sesamol derivatives (Kumar et al., 2021). It was also found that among the cancer cell lines assessed, MCF-7 cells were more sensitive to all the tested sesamol derivatives compounds than A549 and HeLa cells (Kumar et al. 2021).

3.8. Sesamol induced mitochondrial dysfunction and generation of ROS in A459 cells

MMP, crucial indicator of mitochondrial function, can be a characteristic of apoptosis whenever its level drops (Liu et al. 2017). A549 cells exposed to sesamol displayed an apparent reduction in MMP compared to the control samples. Indeed, sesamol significantly caused the loss of MMP to 52.33 ± 8.5 6% at the IC_{50} concentration for 24 h treatment (Fig. 4b).

The ROS level plays a key role in the cellular redox status to regulate cell signaling pathways. Mitochondria is directly involved in controlling cellular redox status by regulation of ROS-mediated signaling pathways (Zhang et al. 2016). As depicted in Fig. 4c, sesamol considerably enhanced the ROS level, which is in good agreement with the MMP loss triggered by sesamol.

Mitochondria are considered as one of the important sources of radical oxygen species (ROS). Indeed, most tumor cells demand a higher level of ROS than normal cells regulate their proliferation (Brillo et al., 2021). The breakable levels of ROS can activate some signaling pathways that are involved in the proliferation of cancer cells. However, excess levels of ROS lead to cell cycle arrest or apoptosis (Arfin et al. 2021). Sesamol triggered mitochondrial dysfunction and promoted ROS level, therefore enhanced oxidative stress in cancer cells.

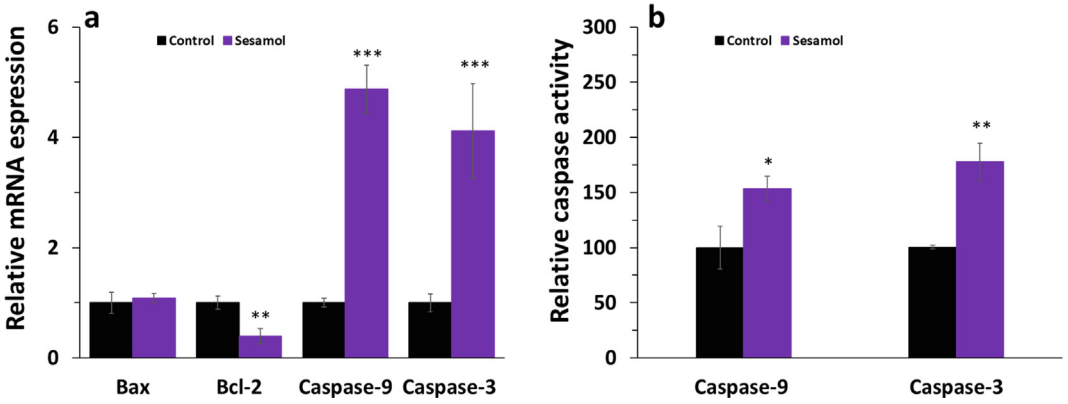

Fig. 5 (a) qPCR assay of A549 lung cancer cells treated with (IC_{50} concentration) of sesamol for 24 h, (b) caspase activity assay of A549 lung cancer cells treated with (IC_{50} concentration) of sesamol for 24 h. Data presented as mean ± SD, n ≥ 3, *P < 0.05, **P < 0.01, ***P < 0.001 versus blank treatment group.

3.9. Sesamol stimulated apoptosis through intrinsic pathway in A549 cells

To investigate the apoptotic mechanism triggered by sesamol, we examined the intrinsic apoptosis pathway. We found that sesamol downregulated the level of anti-apoptotic mRNA Bcl-2, however displayed no impact on the regulation of apoptotic mRNA (Fig. 5a). Also, sesamol enhanced the expression of caspase-9 and caspase-3 at mRNA level (Fig. 5a), which are all main factors that contribute to the induction of intrinsic apoptosis pathway. Simultaneously, sesamol increased the activity of caspase-9 and caspase-3 (Fig. 5b). These results indicated that sesamol reduced cell proliferation through triggering the intrinsic apoptosis in A549 cancer cells.

Previous studies have indicated that mitochondrial quality control is heavily controlled by mitochondrial biogenesis (Kumar Sharma et al. 2022). In this paper, sesamol increased the level of ROS, induced mitochondrial dysfunction, inhibited the expression of antiapoptotic Bcl-2 at mRNA level, and enhanced the mRNA expression and activity of caspase-9,-3, which are consistent with the intrinsic apoptosis-mediated suppression of cancer cells proliferation. Indeed, to inhibit cancer cell proliferation, sesamol was found to have the ability to impair the mitochondria of A549 cells. With the addition of sesamol, we were able to determine that it plays a key role in inhibiting cancer cell growth via regulating the intrinsic apoptosis pathway.

It has been also shown that some other anticancer small molecules including chrysin (Samarghandian et al., 2014), propolis (Frión-Herrera et al., 2015), curcumin derivative (Zhou et al., 2018), and thymol (Balan et al. 2021) can induce anticancer activity against A594 cells via regulation of intrinsic apoptosis pathways mediated by ROS.

4. Conclusion

In the current study, we explored the interaction of HSA with sesamol by different spectroscopic and in silico studies. We found that sesamol binds with HSA with a high affinity and forms a static complex through involvement of hydrogen bonds and van der Waals interaction, which were supported by in silico analyses. It was also found that sesamol can induce apoptosis in A549 cells mediated by reduction of mitochondrial membrane potential and generation of high level of ROS level. Sesamol was able to upregulate the intrinsic apoptosis pathways of apoptosis. Therefore, our study proposes that sesamol can be used as a potential anticancer compound which its function can be regulated by HSA, though some *in vivo* assays and clinical trials are further needed for future studies.

Conflict of interest

None.

Declaration of Competing Interest

The authors declare that they have no known competing financial interests or personal relationships that could have appeared to influence the work reported in this paper.

References

Abd-Algaleel, S.A., Metwally, A.A., Abdel-Bar, H.M., Kassem, D.H., Hathout, R.M., 2021 Aug 30. Synchronizing In Silico, In Vitro, and In Vivo Studies for the Successful Nose to Brain Delivery of an Anticancer Molecule. Mol. Pharm. 18 (10), 3763–3776.

Abd Elrazik, N.A., El-Mesery, M., El-Karef, A., Eissa, L.A., El Gayar, A.M., 2021 Jan. Sesamol upregulates death receptors and acts as a chemosensitizer in solid ehrlich carcinoma model in mice. Nutr. Cancer 3, 1–5.

Abdelaziz, M.A., Shaldam, M., El-Domany, R.A., Belal, F., 2022 Jan. Multi-Spectroscopic, thermodynamic and molecular dynamic simulation studies for investigation of interaction of dapagliflozin with bovine serum albumin. Spectrochim. Acta Part A Mol. Biomol. Spectrosc. 5 (264). 120298.

Abdelhameed, A.S., Bakheit, A.H., Hassan, E.S., Alanazi, A.M., Naglah, A.M., AlRabiah, H., 2022 Apr. Spectroscopic and computational investigation of the interaction between the new anticancer agent enasidenib and human serum albumin. Spectrochim. Acta Part A Mol. Biomol. Spectrosc. 5 (270). 120790.

Abdelhamid, H.N., El-Bery, H.M., Metwally, A.A., Elshazly, M., Hathout, R.M., 2019. Synthesis of CdS-modified chitosan quantum dots for the drug delivery of Sesamol. Carbohydr. Polym. 214, 90–99.

Abdollahpour, N., Soheili, V., Saberi, M.R., Chamani, J., 2016 Dec. Investigation of the interaction between human serum albumin and

two drugs as binary and ternary systems. Eur. J. Drug Metab. Pharmacokinet. 41 (6), 705–721.

Abdolmajid, E., Kharazi, H., Chalaki, M., Khojasteh, M., Haghighat, S., Attar, F., Nemati, F., Falahati, M., 2019 Jul 24. Titanium oxide nanoparticles fabrication, hemoglobin interaction, white blood cells cytotoxicity, and antibacterial studies. J. Biomolecular Structure Dynamics. 37 (11), 3007–3017.

Abou-Zeid, S.M., Elkhadrawey, B.A., Anis, A., AbuBakr, H.O., El-Bialy, B.E., Elsabbagh, H.S., El-Borai, N.B., 2021 Oct. Neuroprotective effect of sesamol against aluminum nanoparticle-induced toxicity in rats. Environ. Sci. Pollution Research. 28 (38), 53767–53780.

Afkham, S., Hanaee, J., Zakariazadeh, M., Fathi, F., Shafiee, S., Soltani, S., 2022 Jan. Molecular mechanism and thermodynamic study of Rosuvastatin interaction with human serum albumin using a surface plasmon resonance method combined with a multi-spectroscopic, and molecular modeling approach. Eur. J. Pharm. Sci. 1 (168). 106005.

Arfin, S., Jha, N.K., Jha, S.K., Kesari, K.K., Ruokolainen, J., Roychoudhury, S., Rathi, B., Kumar, D., 2021 May. Oxidative stress in cancer cell metabolism. Antioxidants. 10 (5), 642.

Arsalan, N., Kashi, E.H., Hasan, A., Doost, M.E., Rasti, B., Paray, B. A., Nakhjiri, M.Z., Sari, S., Sharifi, M., Shahpasand, K., Akhtari, K., 2020. Exploring the interaction of cobalt oxide nanoparticles with albumin, leukemia cancer cells and pathogenic bacteria by multispectroscopic, docking, cellular and antibacterial approaches. Int. J. Nanomed. 15, 4607.

Baghaee, P.T., Divsalar, A., Chamani, J., Donya, A., 2019. Human serum albumin–malathion complex study in the presence of silver nanoparticles at different sizes by multi spectroscopic techniques. J. Biomol. Struct. Dyn. 37 (9), 2254–2264.

Balan, D.J., Rajavel, T., Das, M., Sathya, S., Jeyakumar, M., Devi, K. P., 2021 Feb. Thymol induces mitochondrial pathway-mediated apoptosis via ROS generation, macromolecular damage and SOD diminution in A549 cells. Pharmacol. Rep. 73 (1), 240–254.

Behera, S., Behura, R., Mohanty, P., Sahoo, M., Duggirala, R., 2021. Study of Interaction between Bovine Serum Albumin and Dolutegravir Intermediate: Fluorescence and Molecular Docking Analysis. Biointerface Res. Appl. Chem. 11, 13102–13110.

Beigoli, S., Sharifi Rad, A., Askari, A., Assaran Darban, R., Chamani, J., 2019 Jun 13. Isothermal titration calorimetry and stopped flow circular dichroism investigations of the interaction between lomefloxacin and human serum albumin in the presence of amino acids. J. Biomol. Struct. Dyn. 37 (9), 2265–2282.

Bose, A., 2016 Jan. Interaction of tea polyphenols with serum albumins: A fluorescence spectroscopic analysis. J. Lumin. 1 (169), 220–226.

Bosebabu, B., Cheruku, S.P., Chamallamudi, M.R., Nampoothiri, M., Shenoy, R.R., Nandakumar, K., Parihar, V.K., Kumar, N., 2020 Jul 1. An Appraisal of current pharmacological perspectives of sesamol: a review. Mini Reviews Medicinal Chem. 20 (11), 988–1000.

Brillo, V., Chieregato, L., Leanza, L., Muccioli, S., Costa, R., 2021 Apr. Mitochondrial dynamics, ROS, and cell signaling: A blended overview. Life. 11 (4), 332.

Carter, D.C., He, X.M., Munson, S.H., Twigg, P.D., Gernert, K.M., Broom, M.B., Miller, T.Y., 1989 Jun 9. Three-dimensional structure of human serum albumin. Science 244 (4909), 1195–1198.

ElMasry, S.R., Hathout, R.M., Abdel-Halim, M., Mansour, S., 2018 Dec. In Vitro transdermal delivery of sesamol using oleic acid chemically-modified gelatin nanoparticles as a potential breast cancer medication. J. Drug Delivery Sci. Technol. 1 (48), 30–39.

Frión-Herrera, Y., Díaz-García, A., Ruiz-Fuentes, J., Rodríguez-Sánchez, H., Sforcin, J.M., 2015 Oct. Brazilian green propolis induced apoptosis in human lung cancer A549 cells through mitochondrial-mediated pathway. J. Pharm. Pharmacol. 67 (10), 1448–1456.

Gan, R., Zhao, L., Sun, Q., Tang, P., Zhang, S., Yang, H., He, J., Li, H., 2018 Sep. Binding behavior of trelagliptin and human serum albumin: Molecular docking, dynamical simulation, and multi-spectroscopy. Spectrochim. Acta Part A Mol. Biomol. Spectrosc. 5 (202), 187–195.

Ge, Y.S., Jin, C., Song, Z., Zhang, J.Q., Jiang, F.L., Liu, Y., 2014 Apr. Multi-spectroscopic analysis and molecular modeling on the interaction of curcumin and its derivatives with human serum albumin: A comparative study. Spectrochim. Acta Part A Mol. Biomol. Spectrosc. 24 (124), 265–276.

Hackshaw, A.K., Law, M.R., Wald, N.J., 1997 Oct 18. The accumulated evidence on lung cancer and environmental tobacco smoke. BMJ 315 (7114), 980–988.

Hu, T., Liu, Y., 2015 Mar. Probing the interaction of cefodizime with human serum albumin using multi-spectroscopic and molecular docking techniques. J. Pharm. Biomed. Anal. 25 (107), 325–332.

Jacob, R.B., Andersen, T., McDougal, O.M., 2012 May 31. Accessible high-throughput virtual screening molecular docking software for students and educators. PLoS Comput. Biol. 8 (5). e1002499.

Jendrossek, V., 2012 Jun 1. The intrinsic apoptosis pathways as a target in anticancer therapy. Curr. Pharm. Biotechnol. 13 (8), 1426–1438.

Khamphio, M., Barusrux, S., Weerapreeyakul, N., 2016 Aug. Sesamol induces mitochondrial apoptosis pathway in HCT116 human colon cancer cells via pro-oxidant effect. Life Sci. 1 (158), 46–56.

Kumar, N.Y., Bharathi, K.K., Mudgal, J., VasanthaRaju, S.G., Reddy, S.M., 2021 Jan. Synthesis, characterization of novel Sesamol substituted with thiazolidin-4-one derivatives and their evaluation for anti-oxidant and anti-cancer activities. Results in Chemistry. 1, (3) 100095.

Kumar Sharma, R., Chafik, A., Bertolin, G., 2022. Mitochondrial transport, partitioning and quality control at the heart of cell proliferation and fate acquisition. American Journal of Physiology-Cell. Physiology. Jan 19.

Li, Z., Zhao, L., Sun, Q., Gan, N., Zhang, Q., Yang, J., Yi, B., Liao, X., Zhu, D., Li, H., 2022 Jan. Study on the interaction between 2, 6-dihydroxybenzoic acid nicotine salt and human serum albumin by multi-spectroscopy andmolecular dynamics simulation. Spectrochim. Acta Part A Mol. Biomol. Spectrosc. 10. 120868.

Liu, Z., Xiang, Q., Du, L., Song, G., Wang, Y., Liu, X., 2013 Nov 1. The interaction of sesamol with DNA and cytotoxicity, apoptosis, and localization in HepG2 cells. Food Chem. 141 (1), 289–296.

Liu, Z., Ren, B., Wang, Y., Zou, C., Qiao, Q., Diao, Z., Mi, Y., Zhu, D., Liu, X., 2017 Apr 4. Sesamol induces human hepatocellular carcinoma cells apoptosis by impairing mitochondrial function and suppressing autophagy. Sci. Rep. 7 (1), 1–2.

Ma, X., Wang, J., Hu, G., Chen, Y., Hu, X., Zhu, Y., Ding, L., Ning, S., 2021 Jul 30. Sesamol Epigenetically Induces Estrogen Receptor α Re-expression by Upregulating miR-370-3p in Estrogen Receptor α-Negative Breast Cancer. J. Agric. Food. Chem. 69 (31), 8737–8746.

Macii, F., Biver, T., 2021 Mar. Spectrofluorimetric analysis of the binding of a target molecule to serum albumin: Tricky aspects and tips. J. Inorg. Biochem. 1 (216). 111305.

Mahmoudpour, M., Javaheri-Ghezeldizaj, F., Yekta, R., Torbati, M., Mohammadzadeh-Aghdash, H., Kashanian, S., Dolatabadi, J.E., 2020 Dec. Thermodynamic analysis of albumin interaction with monosodium glutamate food additive: Insights from multi-spectroscopic and molecular docking approaches. J. Mol. Struct. 5, (1221) 128785.

Majdalawieh, A.F., Mansour, Z.R., 2019 Jul. Sesamol, a major lignan in sesame seeds (Sesamum indicum): anti-cancer properties and mechanisms of action. Eur. J. Pharmacol. 15 (855), 75–89.

Maiti, T.K., Ghosh, K.S., Dasgupta, S., 2006 Aug 1. Interaction of (−)-epigallocatechin-3-gallate with human serum albumin: Fluorescence, fourier transform infrared, circular dichroism, and docking studies. Proteins Struct. Funct. Bioinf. 64 (2), 355–362.

McIntyre, A., Ganti, A.K., 2017 Apr. Lung cancer—a global perspective. J. Surg. Oncol. 115 (5), 550–554.
Mealey, K.L., Karriker, M.J., 2019 Apr. Comparative Pharmacokinetics and Pharmacodynamics. Pharmacotherapeutics for Veterinary Dispensing. 2, 75–94.
Nakhjiri, M.Z., Asadi, S., Hasan, A., Babadaei, M.M., Vahdani, Y., Rasti, B., Ale-Ebrahim, M., Arsalan, N., Goorabjavari, S.V., Haghighat, S., Sharifi, M., 2020 Nov. Exploring the interaction of synthesized nickel oxide nanoparticles through hydrothermal method with hemoglobin and lymphocytes: bio-thermodynamic and cellular studies. J. Mol. Liq. 1 (317). 113893.
Qureshi, M.A., Akbar, M., Amir, M., Javed, S., 2022 Jan. Molecular interactions of esculin with bovine serum albumin and recognition of binding sites with spectroscopy and molecular docking. J. Biomol. Struct. Dyn. 31, 1–5.
Salem, A.A., Lotfy, M., Amin, A., Ghattas, M.A., 2019 Dec. Characterization of human serum albumin's interactions with safranal and crocin using multi-spectroscopic and molecular docking techniques. Biochem. Biophys. Rep. 1 (20). 100670.
Samarghandian, S., Azimi Nezhad, M., Mohammadi, G., 2014 Jul 1. Role of caspases, Bax and Bcl-2 in chrysin-induced apoptosis in the A549 human lung adenocarcinoma epithelial cells. Anti-Cancer Agents in Medicinal Chemistry (Formerly Current Medicinal Chemistry-Anti-Cancer Agents) 14 (6), 901–909.
Shimizu, S., Fujii, G., Takahashi, M., Nakanishi, R., Komiya, M., Shimura, M., Noma, N., Onuma, W., Terasaki, M., Yano, T., Mutoh, M., 2014. Sesamol suppresses cyclooxygenase-2 transcriptional activity in colon cancer cells and modifies intestinal polyp development in ApcMin/+ mice. J. Clinical Biochemistry Nutrition. 54 (2), 95–101.
Shroff, G.S., Viswanathan, C., Carter, B.W., Benveniste, M.F., Truong, M.T., Sabloff, B.S., 2018 May 1. Staging lung cancer: metastasis. Radiologic Clinics. 56 (3), 411–418.
Siriwarin, B., Weerapreeyakul, N., 2016 Jul. Sesamol induced apoptotic effect in lung adenocarcinoma cells through both intrinsic and extrinsic pathways. Chem. Biol. Interact. 25 (254), 109–116.
Sułkowska, A., 2002 Sep 2. Interaction of drugs with bovine and human serum albumin. J. Mol. Struct. 614 (1–3), 227–232.
Wang, Y., Zhang, G., Wang, L., 2014 Jan. Interaction of prometryn to human serum albumin: insights from spectroscopic and molecular docking studies. Pestic. Biochem. Physiol. 1 (108), 66–73.
Wang, C., Wu, Q.H., Wang, Z., Zhao, J., 2006. Study of the interaction of carbamazepine with bovine serum albumin by fluorescence quenching method. Anal. Sci. 22 (3), 435–438.
Yeggoni, D.P., Rachamallu, A., Subramanyam, R., 2016 Jul. Protein stability, conformational change and binding mechanism of human serum albumin upon binding of embelin and its role in disease control. J. Photochem. Photobiol., B 1 (160), 248–259.
Zeinabad, H.A., Kachooei, E., Saboury, A.A., Kostova, I., Attar, F., Vaezzadeh, M., Falahati, M., 2016. Thermodynamic and conformational changes of protein toward interaction with nanoparticles: a spectroscopic overview. RSC Adv. 6 (107), 105903–105919.
Zhang J, Wang X, Vikash V, Ye Q, Wu D, Liu Y, Dong W. ROS and ROS-mediated cellular signaling. Oxidative medicine and cellular longevity. 2016 Oct;2016.
Zhou, S., Zou, H., Huang, G., Chen, G., 2021 Jan. Preparations and antioxidant activities of sesamol and it's derivatives. Bioorg. Med. Chem. Lett. 1 (31). 127716.
Zhou, G.Z., Li, A.F., Sun, Y.H., Sun, G.C., 2018 Jul. A novel synthetic curcumin derivative MHMM-41 induces ROS-mediated apoptosis and migration blocking of human lung cancer cells A549. Biomed. Pharmacother. 1 (103), 391–398.
Ziaunys, M., Mikalauskaite, K., Smirnovas, V., 2019 Dec 30. Amyloidophilic molecule interactions on the surface of insulin fibrils: cooperative binding and fluorescence quenching. Sci. Rep. 9 (1), 1.